Single-photon logic gates using minimal resources

Qing Lin[1,*] and Bing He[2,†]
[1]*College of Information Science and Engineering, Huaqiao University (Xiamen), Xiamen 361021, China*
[2]*Institute for Quantum Information Science, University of Calgary, Alberta, Canada T2N 1N4*
(Received 25 June 2009; revised manuscript received 17 August 2009; published 15 October 2009)

We present a simple architecture for deterministic quantum circuits operating on single-photon qubits. Few resources are necessary to implement two elementary gates and can be recycled for computing with large numbers of qubits. The deterministic realization of some key multiqubit gates, such as the Fredkin and Toffoli gate, is greatly simplified in this approach.

DOI: 10.1103/PhysRevA.80.042310 PACS number(s): 03.67.Lx, 42.50.Ex

I. INTRODUCTION

Quantum computing has attracted wide attention for its factoring power and efficient simulation of quantum dynamics. Many efforts have been made in building quantum computers with various physical systems and optical qubits are regarded as a prominent candidate for their robustness against decoherence. An important theoretical breakthrough in the field was the Knill-Laflamme-Milburn (KLM) protocol [1], a circuit-based approach using single-photon sources, single-photon detectors, and linear optical elements. A two-qubit gate could be realized in an asymptotically deterministic way, as the number of photons forming an entangled state for teleportation in the protocol grows to infinity [1,2]. It opens up the possibility of building any quantum logic gate which can be decomposed into two-qubit and single-qubit gates theoretically [3]. The prohibitively large overhead cost of a two-qubit gate in the KLM protocol, however, necessitates various improvements. Most progresses follow in the direction of one way computation [4], an approach imprinting circuits on a particular class of entangled states (cluster states) through measurements. Though it is possible to create cluster states with realistic optical methods [5], the generation of such multiply entangled states is still not efficient with available techniques, imposing a bottleneck on the practical implementation. Beyond linear optics, a near-deterministic controlled-NOT (CNOT) gate based on weak nonlinearities [6] has been proposed and it suggests a way for deterministic quantum computation [7]. In realistic quantum computation, however, it will still require considerable resources to perform a gate involving more than two qubits if one decomposes a complicated quantum circuit into the basic CNOT and single-qubit gates.

An efficient quantum computation approach demanding fewer resources is desirable. In this work, we propose an architecture for quantum logic gates operating on qubits simply encoded as the linear combinations of two single-photon modes, e.g., $|0_L\rangle \equiv |H\rangle$ and $|1_L\rangle \equiv |V\rangle$, where H and V are two polarization modes. In this architecture, a quantum logic gate can be deterministically realized with a combination of two elementary gates. Only one ancilla photon and a few coherent states, which can be recycled after implementing one elementary gate, are necessary to compute with a large number of qubits. Because the qubits and ancillas are in simple quantum states, the operation error of the logic gates would be largely reduced.

II. CONTROLLED-PATH GATE

The first ingredient in our architecture is the controlled-path (C-path) gate introduced in [8]. Here, as shown in Fig. 1, we propose a design with the double cross-phase modulation (XPM) method in [9] to make it more efficient and feasible. This gate performs the following operation on an initial two-photon state $|\psi\rangle_{CT}$ (C stands for the control and T the target):

$$\begin{aligned} |\psi\rangle_{CT} &= a|HH\rangle_{CT} + b|HV\rangle_{CT} + c|VH\rangle_{CT} + d|VV\rangle_{CT} \\ &\rightarrow a|HH\rangle_{C1} + b|HV\rangle_{C1} + c|VH\rangle_{C2} + d|VV\rangle_{C2} \\ &= |\phi\rangle, \end{aligned} \tag{1}$$

where the indices 1 and 2 denote two different paths, implementing the control on the target qubit paths by the polarizations of the control qubit.

In Fig. 1, we first use a 50:50 beam splitter (BS) to divide the target photon T into two spatial modes 1 and 2. Then two

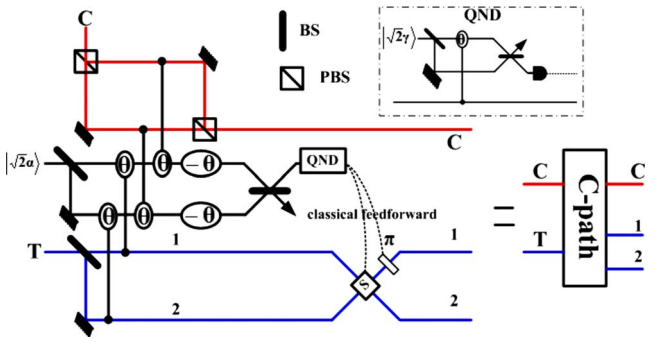

FIG. 1. (Color online) Schematic setup for controlled-path gate. A PBS used in the circuit transmits the mode $|H\rangle$ and reflects the mode $|V\rangle$ of a single photon. Two qubus beams are coupled to the photonic modes as indicated. The XPM phases on the qubus beams θ and two phase shifters $-\theta$ are applied to the qubus beams. The QND module in dash-dotted line is used to perform number-resolving detection.

*qlin@mail.ustc.edu.cn
†bhe98@earthlink.net

 ©2009 The American Physical Society

quantum bus (qubus) beams $|\alpha\rangle|\alpha\rangle$ are introduced, with the first coupling to the target photon mode on path 1 and the $|V\rangle$ mode of the control photon, while the second to the target mode on path 2 and the $|H\rangle$ mode of the control through Kerr media, respectively. Suppose the XPM phase shifts induced in the processes are all θ. After that, a $-\theta$ phase shifter is, respectively, applied to two qubus beams. Finally, one more 50:50 BS implements the transformation $|\alpha_1\rangle|\alpha_2\rangle \rightarrow |\frac{\alpha_1-\alpha_2}{\sqrt{2}}\rangle|\frac{\alpha_1+\alpha_2}{\sqrt{2}}\rangle$, realizing the state

$$\frac{1}{\sqrt{2}}(|H\rangle_C(a|H\rangle_2 + b|V\rangle_2)|-\beta\rangle + |V\rangle_C(c|H\rangle_1 + d|V\rangle_1)|\beta\rangle)|\sqrt{2}\alpha\cos\theta\rangle + \frac{1}{\sqrt{2}}|\phi\rangle|0\rangle|\sqrt{2}\alpha\rangle, \quad (2)$$

where $|\beta\rangle = |i\sqrt{2}\alpha \sin\theta\rangle$. Then, we could use the projections $|n\rangle\langle n|$ on the first qubus beam to get the proper output. If $n=0$, $|\phi\rangle$ will be projected out; on the other hand, if $n\neq 0$, what is realized is $e^{-in(\pi/2)}|H\rangle_C(a|H\rangle_2+b|V\rangle_2) + e^{in(\pi/2)}|V\rangle_C(c|H\rangle_1+d|V\rangle_1)$, which can be transformed to $|\phi\rangle$ by the application of a ± 1 phase factor and the controlled switch of two paths following the classically feed-forwarded measurement results. Since the weak nonlinearity considered here is very small ($\theta \ll 1$), only a small portion of the initial qubus beam $|\sqrt{2}\alpha\rangle$ is consumed by detection; the unmeasured beam in the state $|\sqrt{2}\alpha\cos\theta\rangle$ will be used in the following elementary gates.

After a C-path gate, the target photon will be simultaneously in two different spatial modes depending on the polarizations of the control photon. Therefore, an operation conditioned on the control photon's polarizations can be directly performed on the spatial modes of the target. As we will demonstrate later, this gate offers a way to realize the interaction between multiple photons indirectly.

III. PHOTON NUMBER-RESOLVING DETECTION

The projectors $|n\rangle\langle n|$ required in the C-path gate could be well approximated by a transition edge sensor (TES)—a superconducting microbolometer that has demonstrated very high detection efficiency (95% at $\lambda=1550$ nm) and high photon number resolution [10]. In practice, it is ideal to implement such number-resolving detection with simple devices. Here, we apply the indirect measurement method in [9] for the purpose. It is a quantum nondemolition (QND) module shown inside the dash-dotted line in Fig. 1. The process in the QND module is as follows:

$$|\pm\beta\rangle|\gamma\rangle|\gamma\rangle \rightarrow e^{-|\beta|^2/2}\sum_{n=0}^{\infty}\frac{(\pm\beta)^n}{\sqrt{n!}}|n\rangle|\gamma e^{in\theta}\rangle|\gamma\rangle. \quad (3)$$

With a 50:50 BS, we will obtain a set of coherent-state components $|\frac{\gamma e^{in\theta}-\gamma}{\sqrt{2}}\rangle|\frac{\gamma e^{in\theta}+\gamma}{\sqrt{2}}\rangle$ for $n=0,1,\ldots,\infty$. If the amplitude $|\gamma|$ is large enough, the photon number Poisson distributions of the states $|\frac{\gamma e^{in\theta}-\gamma}{\sqrt{2}}\rangle$ will be separated with negligible overlaps. If the dominant distribution for the component of $n=k$ is from n_k to n_k', we could use a realistic detector described by the following positive-operator-value measurement (POVM) elements to detect $|\frac{\gamma e^{ik\theta}-\gamma}{\sqrt{2}}\rangle$,

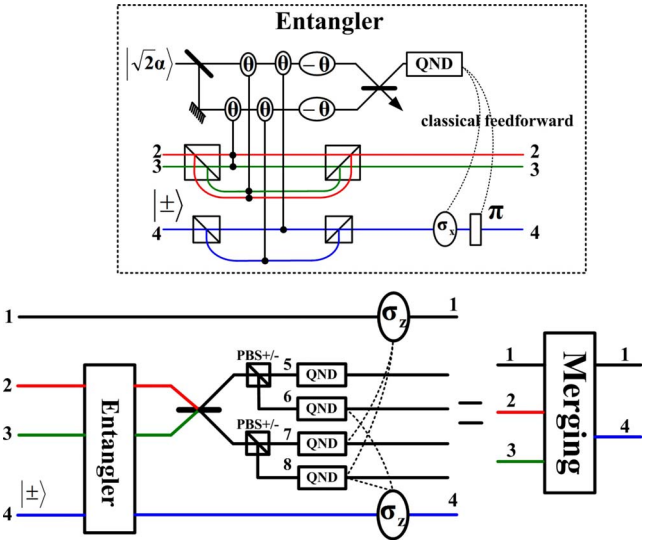

FIG. 2. (Color online) Schematic setup for merging gate. The ancilla photon in the state $|\pm\rangle$. The single-photon modes on paths 2 and 3 interact with the qubus beams in the pattern indicated in entangler. On the first (second) qubus beam, we use one XPM rotation θ to represent the coupling to the $|V\rangle(|H\rangle)$ mode on both paths 2 and 3. A BS and four $\mathrm{PBS}_{\pm}$ divide the modes of the second photon to four paths, on which the QND modules in Fig. 1 are to detect the photon. The operations σ_z are performed according to the feed-forwarded of the QNDs.

$$\Pi_0 = \sum_{n=0}^{\infty}(1-\eta)^n|n\rangle\langle n|,$$

$$\Pi_{n_k} = \sum_{n=n_k}^{n_k'}[1-(1-\eta)^n]|n\rangle\langle n|,$$

$$\Pi_E = I - \Pi_0 - \sum_{k=1}^{\infty}\Pi_{n_k}, \quad (4)$$

where $\eta<1$ is the quantum efficiency of the detector. Π_0 here corresponds to detecting no photon, Π_E to the response to the negligible overlaps, and Π_{n_k} to the reaction to the kth Poisson curve, respectively. The operators Π_{n_k} therefore select out the components $|k\rangle$ in $|\pm\beta\rangle$ indirectly. Physically, Π_{n_k} are the different responses (by the induced currents or voltages) of a number-nonresolving detector to $|\frac{\gamma e^{ik\theta}-\gamma}{\sqrt{2}}\rangle$ of the different intensities.

IV. MERGING GATE

Since the C-path operation splits the target photon into two different paths, we also require a gate to merge these two paths back into a single path. To perform the conversion deterministically, we introduce another elementary gate called the merging gate shown in Fig. 2, where an extra ancilla photon is used. It implements the transformation

$$|\psi\rangle = a|HH\rangle_{12} + b|HV\rangle_{12} + c|VH\rangle_{13} + d|VV\rangle_{13}$$
$$\rightarrow a|HH\rangle_{14} + b|HV\rangle_{14} + c|VH\rangle_{14} + d|VV\rangle_{14}, \quad (5)$$

i.e., the merging of the second photon modes on path 2 and 3 to path 4.

The ancilla photon is in the state $|\pm\rangle = \frac{1}{\sqrt{2}}(|H\rangle \pm |V\rangle)$. A total state $|\psi\rangle|+\rangle$, for example, is first sent to entangler in Fig. 2, where we let the photons interact with the qubus beams (see the setup in the dashed line of Fig. 2). Similar to the double XPM pattern in C-path gate, the total state $|\psi\rangle|+\rangle$ will be transformed to

$$\frac{1}{\sqrt{2}}a|H\rangle_1(|+\rangle_2 + |-\rangle_2)|H\rangle_4 + \frac{1}{\sqrt{2}}b|H\rangle_1(|+\rangle_2 - |-\rangle_2)|V\rangle_4$$
$$+ \frac{1}{\sqrt{2}}c|V\rangle_1(|+\rangle_3 + |-\rangle_3)|H\rangle_4 + \frac{1}{\sqrt{2}}d|V\rangle_1(|+\rangle_3 - |-\rangle_3)|V\rangle_4, \quad (6)$$

with a bit flip σ_x and a phase shifter π conditioned on the results of the number-resolving detection on a qubus beam (no action should be taken if $n=0$). After the interference of the modes on paths 2 and 3, $|\pm\rangle_2 \rightarrow \frac{1}{\sqrt{2}}(|\pm\rangle_2 + |\pm\rangle_3)$ and $|\pm\rangle_3 \rightarrow \frac{1}{\sqrt{2}}(|\pm\rangle_2 - |\pm\rangle_3)$, through a 50:50 BS, two polarization beam splitters in the diagonal basis ($PBS_{\pm}$) let the components $|+\rangle$ be transmitted while having the components $|-\rangle$ reflected, making the single photon run on four different paths numbered from 5 to 8. We then use the QND modules, which are the same as that in Fig. 1, on each path to determine where the single photon in the state $|\pm\rangle$ passes. The QND detections therefore project out the outputs and the projected out photon on one of the paths can be used again in the next merging gate.

V. TWO-QUBIT GATES

Two-qubit gates such as CNOT, controlled-Z (CZ), and C-phase, which are included in the class $|H\rangle\langle H| \otimes U_1 + |V\rangle\langle V| \otimes U_2$, can be simply constructed with these elementary gates. Any gate operation in this form is performed by a C-path gate followed by the single-qubit operations U_1 and U_2 on the different paths of the target photon and then a merging gate. Compared to the qubus mediated CNOT gate in [6], a CNOT gate constructed with a pair of C-path and merging gates uses the same amount of resources—two elementary gates and one ancilla single photon—without counting the QND modules for resolving the photon numbers in a qubus beam and preserving the ancilla photon in detections. Since we apply the double XPM method in [9], the number of the conditional XPM phase rotations in each elementary gate will be greater than that in [6]. In addition to recycling the qubus beams, the advantage of the double XPM method is that a minus XPM phase shift $-\theta$, which is impractical to realize [11], can be avoided. Moreover, unlike the scheme in [7], there is no need for the displacement operations on the qubus beams, which could be hard to implement if the displacement amplitude is large [12,13].

For an arbitrary two-qubit gate $U \in U(4)$, which is expressed as $U=(A_1 \otimes A_2)N(\alpha,\beta,\gamma)(A_3 \otimes A_4)$, where $A_i \in U(2)$ and $N(\alpha,\beta,\gamma)=\exp[i(\alpha\sigma_x \otimes \sigma_x + \beta\sigma_y \otimes \sigma_y + \gamma\sigma_z \otimes \sigma_z)]$ [14], we can diagonalize $N(\alpha,\beta,\gamma)$ to

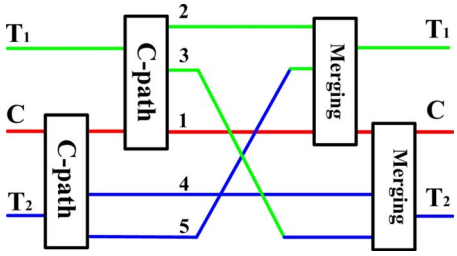

FIG. 3. (Color online) Schematic setup for the Fredkin gate. Two C-path and merging gates, together with the exchange of two path modes, are used to realize a Fredkin gate directly.

$$|H\rangle\langle H| \otimes \mathrm{diag}(e^{i(\alpha-\beta+\gamma)}, e^{-i(\alpha-\beta-\gamma)})$$
$$+ |V\rangle\langle V| \otimes \mathrm{diag}(e^{i(\alpha+\beta-\gamma)}, e^{-i(\alpha+\beta+\gamma)}), \quad (7)$$

with so-called magic transformation $\mathcal{M}$ [15]. The magic transformation, which is equivalent to a CNOT and a few single-qubit operations [15], is also implementable with C-path and merging gates.

VI. MULTIQUBIT GATES

It is straightforward to generalize to multiple qubit gates, as any multiqubit gate is decomposable to a product of two-qubit gates and single-qubit gates [3]. In the framework of realizing quantum computation with the two above-discussed elementary gates, however, the design of a multiqubit gate can be simplified much further. We illustrate the point with two typical multiqubit gates—the Fredkin gate and the Toffoli gate.

The schematic setup in Fig. 3 is a Fredkin gate which implements a swap operation on two target photons controlled by the $|V\rangle$ of the control photon. In other words, it performs the following transformation of a triple photon state $|\Psi\rangle_{CT_1T_2}$:

$$|\Psi\rangle_{CT_1T_2} = A_1|HHH\rangle + A_2|HHV\rangle + A_3|HVH\rangle + A_4|HVV\rangle$$
$$+ A_5|VHH\rangle + A_6|VHV\rangle + A_7|VVH\rangle + A_8|VVV\rangle$$
$$\rightarrow A_6|VVH\rangle + A_7|VHV\rangle + rest\,., \quad (8)$$

where *rest*. denotes the unchanged terms. Here, we use two C-path gates to map the second photon to paths 2 and 3 and the third photon to paths 4 and 5

$$|H\rangle_1(A_1|HH\rangle + A_2|HV\rangle + A_3|VH\rangle + A_4|VV\rangle)_{24}$$
$$+ |V\rangle_1(A_5|HH\rangle + A_6|HV\rangle + A_7|VH\rangle + A_8|VV\rangle)_{35}. \quad (9)$$

A deterministic Fredkin gate can be therefore realized by exchanging the modes on paths 3 and 5 and using two merging gates as the inverse operation of two C-path gates. In the implementation of two merging gates, only one ancilla photon is necessary since it can be used again after QND detection. This feature is especially useful when there are many merging gates in computation.

The Toffoli gate illustrated in Fig. 4 is the bit flip of a target photon conditioned on both $|V\rangle$ of two control photons,

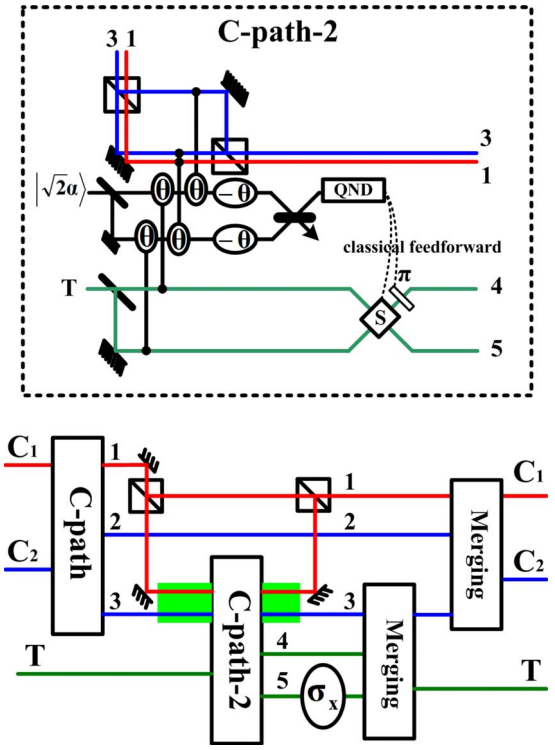

FIG. 4. (Color online) Schematic setup for Toffoli gate. The H mode of photon C_1 and the modes on path 3 after the first C-path gate control the target photon in the second C-path gate. A bit flip is performed on the target mode on path 5. The couplings of the qubus beams with the relevant photonic modes in C-path 2 are illustrated in dashed line. On the second qubus beam of the C-path 2 gate, we use one XPM rotation θ to represent the couplings to both $|H\rangle$ modes of paths 1 and 3.

i.e., a triple-qubit operation $(I\otimes I-|VV\rangle\langle VV|)\otimes I+|VV\rangle\langle VV|\otimes\sigma_x$, where $I=|H\rangle\langle H|+|V\rangle\langle V|$. To implement the gate, we start with a C-path gate for the initial state $|\Psi\rangle_{C_1C_2T}$ [in the same form as $|\Psi\rangle_{C_1T_1T_2}$ in Eq. (8)] to send the second photon C_2 to two different paths 2 and 3 under the control of the polarizations of the first photon C_1,

$$|\Psi\rangle_{C_1T_1T_2}\rightarrow(A_1|HHH\rangle+A_2|HHV\rangle+A_3|HVH\rangle+A_4|HVV\rangle)_{12T}+(A_5|VHH\rangle+A_6|VHV\rangle+A_7|VVH\rangle+A_8|VVV\rangle)_{13T}=|\Psi_1\rangle. \quad (10)$$

Meanwhile, as shown in dashed line of Fig. 4, a 50:50 BS divides the target photon T into two paths 4 and 5. Two qubus beams $|\alpha\rangle|\alpha\rangle$ will be applied to perform the second C-path gate with the control of the modes $|H\rangle_3$ and $|V\rangle_3$ on path 3. There is a slight difference in this C-path gate (denoted as C-path 2 in Fig. 4) from a standard one in Fig. 1—the second beam is coupled not only to the mode on path 5 and the $|H\rangle$ mode on path 3 but also to $|H\rangle_1$ of the first control photon, while the first beam interacts with the target mode on path 4 and the $|V\rangle$ control mode on path 3, as indicated in the following transformation:

$$\begin{aligned}|\Psi_1\rangle|\alpha\rangle|\alpha\rangle\rightarrow&\frac{1}{\sqrt{2}}|HH\rangle_{12}\{(A_1|H\rangle_4+|A_2|V\rangle_4)|\alpha e^{i\theta},\alpha e^{i\theta}\rangle\\&+(A_1|H\rangle_5+|A_2|V\rangle_5)|\alpha,\alpha e^{i2\theta}\rangle\}\\&+\frac{1}{\sqrt{2}}|HV\rangle_{12}\{(A_3|H\rangle_4+|A_4|V\rangle_4)|\alpha e^{i\theta},\alpha e^{i\theta}\rangle\\&+(A_3|H\rangle_5+|A_4|V\rangle_5)|\alpha,\alpha e^{i2\theta}\rangle\}\\&+\frac{1}{\sqrt{2}}|VH\rangle_{13}\{(A_5|H\rangle_4+|A_6|V\rangle_4)|\alpha e^{i\theta},\alpha e^{i\theta}\rangle\\&+(A_5|H\rangle_5+|A_6|V\rangle_5)|\alpha,\alpha e^{i2\theta}\rangle\}\\&+\frac{1}{\sqrt{2}}|VV\rangle_{13}\{(A_7|H\rangle_4+|A_8|V\rangle_4)|\alpha e^{i2\theta},\alpha\rangle\\&+(A_7|H\rangle_5+|A_8|V\rangle_5)|\alpha e^{i\theta},\alpha e^{i\theta}\rangle\}. \quad (11)\end{aligned}$$

The remaining operations on two qubus beams are the same as those in a standard C-path gate—two phase shifts $-\theta$ and a 50:50 BS. According to the number-resolving detection results on one qubus beam, an output state,

$$|H\rangle_1(A_1|HH\rangle+A_2|HV\rangle+A_3|VH\rangle+A_4|VV\rangle)_{24}+|VH\rangle_{13}(A_5|H\rangle+A_6|V\rangle)_4+|VV\rangle_{13}(A_7|H\rangle+A_8|V\rangle)_5, \quad (12)$$

will be deterministically projected out. After that, a bit flip σ_x is performed on path 5 alone. The total operation for a deterministic Toffoli gate will be then completed with two merging gates for the modes on paths 4 and 5 and on paths 2 and 3, respectively.

This design can be generalized to the situation of more than three qubits, where we could simply adopt the similar coupling patterns for the photonic modes in the successive C-path gates. In Fig. 5, we outline a triple-control Toffoli gate of such type, which implements the bit flip of a target photon under the $|V\rangle$ modes of three control photons together. The simplicity of this approach stands out as compared to the conventional method of decomposing a quantum circuit into double-qubit and single-qubit gates. By the conventional method, there should be at least five two-qubit gates for the Fredkin and Toffoli gates [16]. Here, we deterministically realize them with only two pairs of C-path and merging gates, which are equivalent to two double-qubit gates. Generally, there should be $O(n^2)$ two-qubit gates to simulate a multicontrol gate of n qubits in the decomposition approach [17]. As shown in Figs. 4 and 5, however, we will only need a number of the elementary gates, which grows linearly with the number of the involved qubits, to realize a multicontrol gate. The decomposition of a multiqubit circuit into two-qubit and single-qubit gates is also theoretically complicated. But in our approach, the construction of a multicontrol gate follows a regular way as from Figs. 4 and 5.

VII. EXPERIMENTAL FEASIBILITY

Here, we take a brief look at the feasibility of this quantum computation approach. A core technique for realizing the

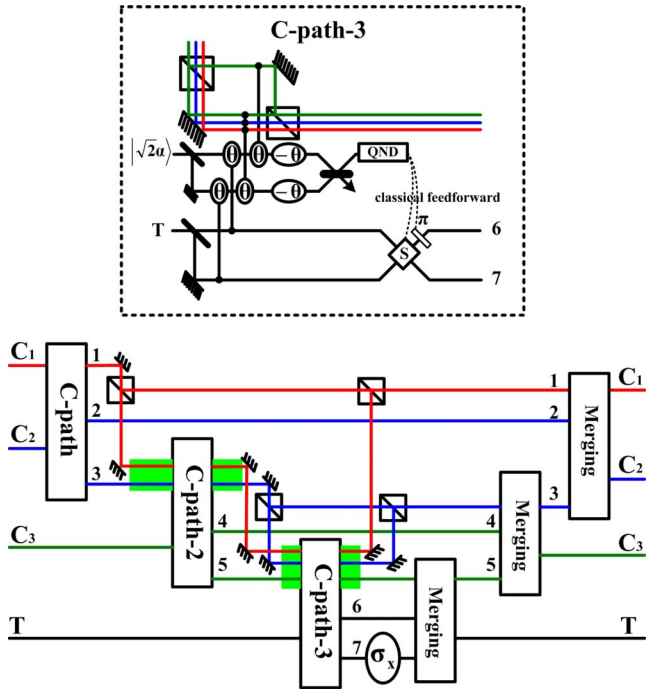

FIG. 5. (Color online) Schematic setup for a triple-control Toffoli gate, with the $|V\rangle$ modes of three photons from C_1 to C_3 controlling the bit flip σ_x on the target photon T. As a simple generalization of the design in Fig. 4, it applies another modified C-path gate—C-path 3—illustrated in dashed line. On the second qubus beam of the C-path 3 gate, we use just one XPM rotation θ to represent the couplings to the $|H\rangle$ mode of paths 1, 3, and 5, respectively. Only one ancilla photon will be necessary for the three merging gates if we apply the detections with QND modules.

elementary gates is the XPM in Kerr media. Good candidates for weak cross-Kerr nonlinearity without self-phase modulation effects are atomic systems working under electromagnetically induced transparency (EIT) conditions [18]. With light-storage technique, for example, it is possible to realize a considerable XPM phase shift at the single-photon level [19]. In principle, however, we only need a small XPM phase shift which can be compensated by the large amplitude of the qubus beams as in [6,7]. The error probability of a detection in the QND modules is

$$\left\| \sum_{n=0}^{\infty} e^{-|\beta|^2/2} \frac{(\pm\beta)^n}{\sqrt{n!}} |n\rangle \left(\Pi_0^{1/2} \left| \frac{\gamma e^{in\theta} - \gamma}{\sqrt{2}} \right\rangle \right) \right\|^2 \sim \exp\{-2(1 - e^{-1/2\eta\gamma^2\theta^2})\alpha^2 \sin^2\theta\}, \quad (13)$$

rendering a near-deterministic performance given $|\alpha|\sin\theta \gg 1$. Moreover, there is no XPM phase shift $-\theta$ and no displacement operation on the qubus beams. The design is robust against small losses of the photonic modes in the double XPM processes [13] and is workable with the realistic number-nonresolving detectors as we apply the indirect detection of photon numbers.

VIII. SUMMARY

The architecture of a quantum computer based on two elementary gates—controlled-path gate and merging gate—is relatively simple compared to those of all other approaches. The data to be processed is directly encoded in single-photon modes and the ancilla photon and communication beams are also in simple quantum states so that the possibility for operational errors could be minimized. The recyclable ancillas keep the resources required in multiqubit computing minimal. Such quantum computer may come into being with the development of the techniques of cross-Kerr nonlinearity and quantum memory for single-photon qubits.

ACKNOWLEDGMENTS

B.H. thanks C. F. Wildfeuer for helpful discussion on photon number-resolving detections and the partial support from iCORE.

[1] E. Knill *et al.*, Nature (London) **409**, 46 (2001).
[2] E. Knill, Phys. Rev. A **68**, 064303 (2003); T. B. Pittman, B. C. Jacobs, and J. D. Franson, Phys. Rev. Lett. **88**, 257902 (2002); J. L. O'Brien *et al.*, Nature (London) **426**, 264 (2003).
[3] M. A. Nielsen and I. L. Chuang, *Quantum Computation and Quantum Information* (Cambridge University Press, Cambridge, England, 2000).
[4] R. Raussendorf and H. J. Briegel, Phys. Rev. Lett. **86**, 5188 (2001); M. A. Nielsen, *ibid.* **93**, 040503 (2004); D. E. Browne and T. Rudolph, *ibid.* **95**, 010501 (2005).
[5] P. Kok *et al.*, Rev. Mod. Phys. **79**, 135 (2007).
[6] K. Nemoto and W. J. Munro, Phys. Rev. Lett. **93**, 250502 (2004).
[7] W. J. Munro *et al.*, New J. Phys. **7**, 137 (2005); T. P. Spiller *et al.*, *ibid.* **8**, 30 (2006).
[8] Q. Lin and J. Li, Phys. Rev. A **79**, 022301 (2009).
[9] B. He, Y. Ren, and J. A. Bergou, Phys. Rev. A **79**, 052323 (2009).
[10] A. J. Miller *et al.*, Appl. Phys. Lett. **83**, 791 (2003); A. E. Lita *et al.*, Opt. Express **16**, 3032 (2008); C. F. Wildfeuer, A. Pearlman, J. Chen, J. Fan, A. Migdall, and J. Dowling, e-print arXiv:0905.1085.
[11] P. Kok, Phys. Rev. A **77**, 013808 (2008).
[12] M. G. Paris, Phys. Lett. A **217**, 78 (1996).
[13] B. He, M. Nadeem, and J. A. Bergou, Phys. Rev. A **79**, 035802 (2009).
[14] N. Khaneja, R. Brockett, and S. J. Glaser, Phys. Rev. A **63**, 032308 (2001); B. Kraus and J. I. Cirac, *ibid.* **63**, 062309 (2001); J. Zhang, J. Vala, S. Sastry, and K. B. Whaley, *ibid.* **67**, 042313 (2003).
[15] F. Vatan and C. Williams, Phys. Rev. A **69**, 032315 (2004).
[16] J. A. Smolin and D. P. DiVincenzo, Phys. Rev. A **53**, 2855 (1996).
[17] A. Barenco, C. H. Bennett, R. Cleve, D. P. DiVincenzo, N. Margolus, P. Shor, T. Sleator, J. A. Smolin, and H. Weinfurter, Phys. Rev. A **52**, 3457 (1995).
[18] H. Schmidt and A. Imamoglu, Opt. Lett. **21**, 1936 (1996); M. Fleischhauer *et al.*, Rev. Mod. Phys. **77**, 633 (2005).
[19] Y.-F. Chen, C. Y. Wang, S. H. Wang, and I. A. Yu, Phys. Rev. Lett. **96**, 043603 (2006).